ISSN 1330-3651 (Print), ISSN 1848-6339 (Online)
https://doi.org/10.17559/TV-20250303002436
Original scientific paper

Effects of Heat Flux and Ignition Type on the Combustion of Live *Pinus nigra* Branches

Milan PROTIĆ*, Nikola MIŠIĆ, Miomir RAOS*, Viša TASIĆ, Dušan TOPALOVIĆ

Abstract: This study investigates the influence of ignition type (piloted and unassisted) and heat flux levels on the combustion behaviour and gas products emissions of live *Pinus nigra* terminal branches. Samples were exposed to three heat flux levels (50, 60, and 70 kW/m^2) using an adapted mass loss calorimeter coupled with an FTIR gas analyzer to simultaneously monitor flammability parameters and combustion product concentrations in real time. Results demonstrated that piloted ignition significantly reduced ignition times and enhanced heat release rates compared to unassisted ignition, particularly at lower heat fluxes. However, at 70 kW/m^2, differences between ignition types diminished, indicating that higher incident radiant energy alone was sufficient to initiate flaming combustion. Combustion product analysis revealed that CO_2, NO, CH_4, and C_2H_4 concentrations followed heat release rate trends. During piloted ignition, higher concentrations of CO_2 and NO and lower emissions of CO and CH_4 were observed compared to unassisted ignition. Principal Component Analysis showed the combined effect of heat flux and ignition type on combustion efficiency and gas composition. These findings highlight the importance of ignition mechanisms in understanding vegetation flammability, providing valuable data for wildfire behaviour modeling and fire safety assessments.

Keywords: combustion; effluents characterization; FTIR, ignition; mass loss cone; wildland fires

1 INTRODUCTION

Forest fires have been increasing globally due to a combination of climate change, shift in land-management, and human activities [1]. Higher global temperatures and longer drought conditions have caused vegetation to dry out, increasing the likelihood of forest fuel ignitions. Additionally, the spread of human populations into areas near wildlands has significantly contributed to the growing frequency and intensity of wildfires. Human activities in this wildland-urban interface, such as agricultural burns, accidental ignitions, and the presence of power lines, have further escalated the occurrence and severity of wildfires. This trend is particularly pronounced in North America. In recently published study [2], the average annual burned areas across the world are reported. From 1992 to 2020, the average annual extent of burned land in the United States was approximately 24,700 km^2, while Australia experienced significantly larger affected regions, averaging around 450,000 km^2 between 2001 and 2020. During the same period, Europe recorded an average yearly burn area of about 3,400 km^2 [2]. Predictions regarding future forest fires are far from optimistic. According to [3], projections based on an ensemble of global climate models suggest that the number of wildfires may triple by 2050.

The increasing frequency and devastating effects of wildfires have led to rapidly growing interest in wildfire research. Rothermel's basic surface fire spread model [4], proposed in the 1970s, is considered the first scientifically rigorous model that closely aligned with experimental results. Although newer technologies have been introduced, this model continues to be widely used in contemporary fire management applications and decision-making frameworks such as BehavePlus [5], FlamMap [6], and FireFamily Plus [7].

Understanding the flammability properties of vegetation is essential for precise wildfire spread modeling, as the characteristics of ignition, burning behavior, and heat output from fuels directly impact the dynamics of fire spread and the predictions made by models. Flammability of forest and wildland vegetation is widely covered in literature. Studies have extensively examined mostly fine dead and dried fuels, analyzing their moisture content, physiological and morphological traits, and combustion dynamics [8-12]. Additionally, the literature review revealed that, although to a lesser extent, there are studies addressing shoot and bark flammability [13-17]. The influence of ignition methods on fuel combustion (ignition times, flame development, and overall fire behavior) has also been a subject of considerable interest [18, 19]. These analyses are important for advancing fire models and increasing the credibility of predictions. Finally, there are also studies analyzing emissions during the combustion of forest fuels [20-22]. Understanding the emissions from live fuel combustion is vital, as these effluents significantly impact atmospheric chemistry, air quality, and human health.

However, comprehensive analyses that integrate flammability characteristics with the evaluation of combustion products in live fuels are scarce. The unique properties of live fuels, including higher moisture content and living tissues, considerably influence their combustion behavior and require further investigation. This study addresses this gap by analyzing the flammability characteristics and combustion effluents of live *Pinus nigra* branches under varying heat flux levels and ignition types. *Pinus nigra* was selected for its extensive distribution in Southern and Central Europe, the Eastern Mediterranean, and Northwestern Africa. By combining flammability analysis with combustion product characterization, the research provides valuable insights into the fire behavior of *Pinus nigra* and its potential contribution to wildfire spread, supporting the development of effective wildfire management and prevention strategies. This article substantially extends our previous conference communication [23].

2 MATERIALS AND METHODS

2.1 Sample Preparation and Testing Procedure

Flammability experiments were performed on terminal shoots of branches from the crown of the coniferous species *Pinus nigra*, collected from the forests surrounding the Vlasina lake in Serbia in July 2023. The terminal shoots

were clipped to approximately the same length, around 13 ±0.5 cm. Immediately after collection, the samples were packed in hermetically sealed bags to minimize moisture loss before testing. To determine the moisture content of the samples, a control group of five samples was separated and dried to a constant weight in an oven at a temperature of 60 °C. The samples were weighed before and after drying using a Radwag analytical balance (AS 60/220.R2, Poland). An average moisture content of 120 ± 10% was determined.

Experiments to determine ignitibility characteristics were conducted at the Fire Protection Laboratory of the Faculty of Occupational Safety, University of Niš, Serbia. The testing setup consisted of a Mass Loss Calorimeter with chimney (Fire Testing Technology, UK), placed in a specially designed fume hood connected to a flue gas extraction system designed in accordance with ISO 5660-1:2015 [24]. A part of the flue gases/fire effluents generated during the flammability experiment was diverted through the heated gas extraction line and connected to an FTIR gas analyzer (Gasmet, FI) for online analysis. The entire setup, as well as the calibration procedure, is described in detail in our previous work [25].

To guarantee proper exposure of the samples to the designated heat flux while minimizing the impact of the standard mass calorimeter sample holder, a custom-designed holder measuring 13 × 13 cm with a porosity exceeding 80% was used. This configuration facilitated unobstructed airflow through the sample holder and limited its effect on the measurements. All samples were carefully trimmed to fit within the holder's boundaries.

2.2 Experimental Design

A full factorial experiment was conducted, covering all possible combinations of the investigated factor levels. The factors and levels are presented in Tab. 1.

Table 1 Factors and levels in experimental design

Factor	Unit	Level 1	Level 2	Level 3
Heat flux	kW/m^2	70	60	50
Ignition type	-	PI ON	PI OFF	-
Plant species	-	*P. nigra*		

Piloted ignition (designated as PI ON) comprises the use of a conical heater and spark igniter to initiate combustion once the lower flammability limit of volatile compounds and air is reached just above the fuel. This scenario simulates ignition sources such as firebrands or other burning particles. In contrast, unpiloted ignition (designated as PI OFF) occurs without an igniter. In this case, the sample is exposed solely to heat flux, causing the fuel-air mixture to ignite when a sufficiently high temperature is reached. Hence, proposed approach enables the examination of differences in ignitibility parameters and combustion product composition under varying ignition mechanisms of forest vegetation.

The first experimental factor was the heat flux (Factor A), with three levels: 50, 60, and 70 kW/m^2. The second factor was the type of ignition (Factor B), with two levels: piloted ignition (PI-ON) and unpiloted ignition (PI-OFF). The study was based on a 3 × 2 factorial design, covering all possible combinations of factor levels. Hence, there were six treatment combinations, with each combination repeated at least five times. The experiments were conducted in a controlled environment with constant temperature and humidity to minimize external influences on the experimental results. During the experiments, the following dependent variables (flammability parameters) were measured and recorded: Time to Ignition (TTI), Mean Heat Release Rate (Mean HRR), Peak Heat Release Rate (PHRR), Peak Effective Heat of Combustion (Peak EHC), Mass Loss Rate (MLR), and Total Heat Release (THR).

The composition of combustion products was analyzed using an FTIR gas analyzer. The concentrations of the following chemical species were continuously measured: water vapor (H_2O), carbon dioxide (CO_2), carbon monoxide (CO), nitrogen monoxide (NO), nitrogen dioxide (NO_2), ammonia (NH_3), methane (CH_4), and ethylene (C_2H_4). Other compounds were either not identified or were present at concentrations below the instrument's detection limit.

2.3 Statistical Analysis

First, the normality of the data distribution was tested. The results of the Shapiro-Wilk test showed that the data followed a normal distribution. Afterward, an independent samples t-test was conducted to evaluate the differences in average flammability characteristics and the composition of combustion products between piloted and unpiloted ignition at a specified heat flux level. A two-way ANOVA was used to analyze the effect of different combinations of heat flux levels and ignition types on these parameters. This analysis also provides insight into the interaction between the two factors, offering a comprehensive understanding of their impact on the dependent variables. Principal Component Analysis (PCA) was applied to determine the effect of ignition type on the interdependence of flammability parameters and combustion products at each heat flux level. PCA biplots were generated to visualize the clustering of experimental sample groups subjected to piloted and unpiloted ignition, enabling the identification of underlying patterns and correlations between the measured variables and their contribution to specific sample groups. For all statistical tests, the significance level (α) was set at 95%. The statistical analysis was performed using R software (RStudio IDE).

3 RESULTS AND DISCUSSION

3.1 Interaction of Heat Flux and Ignition Type on Flammability Parameters

Three characteristic combustion phases were observed during the experiments. After placing the samples, the first phase involved devolatilization, during which moisture and easily volatile compounds were released from the sample. Upon reaching the lower flammability limit, ignition occurred, marking the beginning of the second phase, flaming combustion. The visible flame area increased as heat accelerated the release of volatile compounds. The flame remained active as long as the concentration of volatiles stayed within the flammability limits. After flame extinction, the third phase, known as glowing combustion, began, characterized by the combustion of the remaining carbon in the sample. The duration of these phases varied

depending on the type of fuel, heat flux, and moisture content. However, in some cases during unassisted ignition, the flaming phase was not observed.

Tab. 2 presents the obtained experimental results, along with the statistical findings from the independent samples t-test and the two-way ANOVA analysis. For all statistical analysis, level of significance was set to standard value $\alpha = 0.05$.

The two-way ANOVA showed statistically significant results ($p < 0.05$) in most cases across all combinations involving the experimental factors and flammability parameters, as well as for the interaction between the experimental factors (A × B). However, no statistically significant effect was found for the mean MLR due to changes in heat flux levels ($p > 0.05$). Additionally, the t-test indicated that the results for all analyzed flammability parameters were not statistically significant for the group of experimental units exposed to a heat flux of 70 kW/m² ($p > 0.05$). Similarly, the results for the mean MLR and THR were not statistically significant for the group of experimental units exposed to a heat flux of 60 kW/m^2. The obtained results suggested that heat flux levels of 60 and 70 kW/m^2, as well as the ignition type (piloted or unpiloted), did not have a statistically significant effect on most of the analyzed flammability parameters.

Table 2 Experimental and statistical results of the interaction between heat flux and ignition type on flammability parameters

Heat flux (Factor A)	Ignition type (Factor B)	Flammability parameters					
		TTI / s	*t*-test *p*-value	Mean HRR / kW/m^2	*t*-test *p*-value	PHRR / kW/m^2	*t*-test *p*-value
50 kW/m^2	PI ON	114.14 ± 17.8	**0.000**	176.26 ± 15.1	**0.000**	229.76 ± 16.5	**0.000**
	PI OFF	No ignition		62.29 ± 10.3		138.29 ± 13.8	
60 kW/m^2	PI ON	76.13 ± 22.8	**0.000**	159.05 ± 14	**0.000**	210.29 ± 21.8	**0.001**
	PI OFF	No ignition		68.61 ± 13.2		141.17 ± 12.3	
70 kW/m^2	PI ON	67.56 ± 12.3	0.052	131.21 ± 12.4	0.907	169.17 ± 12.2	0.295
	PI OFF	83.83 ± 12.2		131.05 ± 21.6		156.68 ± 23.7	
Two-way ANOVA results		***p*-value**		***p*-value**		***p*-value**	
Heat flux (Factor A)		**0.000**		**0.018**		**0.012**	
Ignition type (Factor B)		**0.000**		**0.000**		**0.000**	
Interaction (A × B)		**0.000**		**0.000**		**0.000**	

Table 2 (cont'd)

Heat flux (Factor A)	Ignition type (Factor B)	Flammability parameters					
		Mean MLR / g/s	*t*-test *p*-value	THR / MJ/m^2	*t*-test *p*-value	Peak EHC / MJ/kg	*t*-test *p*-value
50 kW/m^2	PI ON	0.081 ± 0.04	**0.011**	7.43 ± 1.8	**0.049**	36.11 ± 16.5	**0.022**
	PI OFF	0.02 ± 0.005		11.53 ± 2.4		63.04 ± 8	
60 kW/m^2	PI ON	0.064 ± 0.04	0.146	6.50 ± 2	0.150	28.70 ± 16.2	**0.038**
	PI OFF	0.03 ± 0.004		9.26 ± 1.5		54.68 ± 15	
70 kW/m^2	PI ON	0.05 ± 0.01	0.533	7.34 ± 1.2	0.169	33.58 ± 13.1	0.831
	PI OFF	0.05 ± 0.02		5.97 ± 1.7		38.01 ± 7.4	
Two-way ANOVA results		***p*-value**		***p*-value**		***p*-value**	
Heat flux (Factor A)		0.729		**0.001**		**0.021**	
Ignition type (Factor B)		**0.000**		**0.002**		**0.000**	
Interaction (A × B)		**0.004**		**0.001**		**0.034**	

The results in Tab. 2 indicate that when a spark igniter was used, the samples ignited at all three heat flux levels. For piloted ignition, the TTI was 114.14 ± 17.8, 76.13 ± 22.8, and 67.56 ± 12.3 seconds at heat flux levels of 50, 60, and 70 kW/m^2, respectively. As expected, the shortest ignition time was recorded at a heat flux of 70 kW/m^2. In contrast, when the spark igniter was not applied, the samples did not ignite at heat fluxes of 50 and 60 kW/m^2. In these cases, only visible thermal degradation/devolatilization of the samples occurred without the formation of a flame. This may be attributed to the presence of moisture in the samples, which is released as water vapor under thermal radiation. The released water vapor dilutes the volatile compounds in the reaction zone, preventing the concentration required to initiate ignition solely from the radiant heater, without the use of a spark igniter. Ignition was observed only at a heat flux of 70 kW/m^2 and in this case ignition time was 83.83 ± 12.2 seconds.

Fig. 1 shows the HRR development for piloted and unpiloted ignition at incident heat fluxes of 50, 60, and 70 kW/m^2. In the experiments where a flaming phase was observed, the HRR rapidly increased to its maximum value at the moment close to the sample ignition. The peak HRR was reached as a result of the previously attained peak MLR, since the intensity of heat generation was directly related to the amount of volatile compounds emitted during the thermal degradation of the samples. Immediately afterward, the HRR value sharply decreased due to the consumption of the samples until the flame was extinguished. In contrast, during unpiloted ignition, the HRR curve did not exhibit a sharp increase, and its peak value was less pronounced. This difference indicated that piloted ignition enabled a faster and more intense combustion process, as the presence of a spark igniter facilitated the initiation of the flaming phase. In contrast, during unpiloted ignition, the energy was emitted at a slower pace, effect that was especially noticeable at reduced heat flux levels.

The time required to reach the PHRR was shorter for piloted ignition compared to unpiloted ignition at all heat flux levels (50, 60, and 70 kW/m^2). At a heat flux of 50 kW/m^2, the average time to reach PHRR was 117 seconds for piloted ignition, whereas for unpiloted ignition, it was longer and occurred at 133.8 seconds. This difference was also present at higher heat flux levels. At 60 kW/m^2, piloted ignition took 92 seconds compared to 109 seconds for unpiloted ignition. At 70 kW/m^2, the difference was even

more pronounced - 66 seconds for piloted ignition versus 88 seconds for unpiloted ignition.

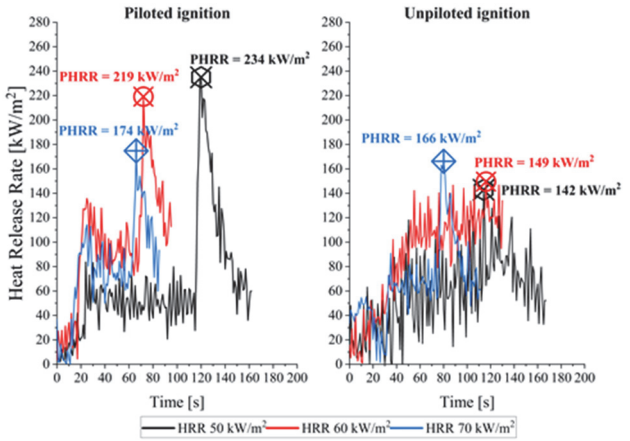

Figure 1 Graphical representation of HRR development for piloted and unpiloted ignition at incident heat fluxes of 50, 60, and 70 kW/m² [23]

Based on the results from Tab. 2, the PHRR decreased with increasing heat flux, from 229.76 kW/m² at 50 kW/m² to 210.29 kW/m² at 60 kW/m², and further down to 169.17 kW/m² at 70 kW/m². In contrast, for unpiloted ignition, the PHRR values were significantly lower compared to piloted ignition at all heat flux levels. Unlike piloted ignition, the PHRR value increased with rising heat flux, with the highest recorded value being 156.68 kW/m² at a heat flux of 70 kW/m². A comparison of the results for piloted and unpiloted ignition using the t-test showed statistically significant differences in the mean HRR and PHRR for the experimental sample group exposed to heat fluxes of 50 and 60 kW/m². However, at a heat flux of 70 kW/m², the results indicated no statistically significant differences between the two ignition types.

At heat fluxes of 50 and 60 kW/m², significantly higher values of the mean HRR and PHRR were observed during piloted ignition compared to unpiloted ignition. This difference indicated a more intense and faster combustion process enabled by the use of a spark igniter. The t-test confirmed that there were statistically significant differences in the mean HRR and PHRR values at these heat flux levels. On the other hand, at a heat flux of 70 kW/m², the results indicated no statistically significant differences between the two ignition types. This suggested that at high heat flux levels, the radiant energy was sufficient to initiate flaming combustion even without the spark igniter.

MLR was higher during the initial stages of combustion under piloted ignition compared to unpiloted ignition, with this trend being particularly pronounced at heat fluxes of 50 and 60 kW/m². In unpiloted ignition, the MLR was significantly slower and exhibited a more gradual decline, which was noticeable at the lower heat flux levels of 50 and 60 kW/m². At a heat flux of 70 kW/m², the differences in MLR values between piloted and unpiloted ignition became less pronounced.

The outcomes of the t-test showed a statistically significant difference at a heat flux of 50 kW/m², where piloted ignition exhibited a significantly higher mean MLR compared to unpiloted ignition. In contrast, at heat flux levels of 60 and 70 kW/m², the differences between the two ignition types were not statistically significant. This suggested that the influence of the ignition type was most pronounced at lower levels of thermal radiation (50 kW/m²), while at higher heat flux values (60 and 70 kW/m²), the differences in the MLR became negligible.

Figure 2 presents the results for THR and peak EHC. The THR values for unpiloted ignition were significantly higher at heat fluxes of 50 and 60 kW/m² compared to piloted ignition, although the difference decreased at a heat flux of 70 kW/m². The t-test confirmed a statistically significant difference in THR values between piloted and unpiloted ignition at a heat flux of 50 kW/m², which was not the case at other heat flux levels. The highest THR value, with an average of 11.53 MJ/m², was recorded during unpiloted ignition at a heat flux of 50 kW/m². On the other hand, the lowest THR value was also observed during unpiloted ignition at a heat flux of 70 kW/m², with an average value of 5.67 MJ/m². Similar differences were observed in the values of peak EHC. The results at heat fluxes of 50 and 60 kW/m² showed significantly higher values for unpiloted ignition compared to piloted ignition, which was confirmed by the *t*-test, indicating that the differences were statistically significant. However, this was not the case at a heat flux of 70 kW/m².

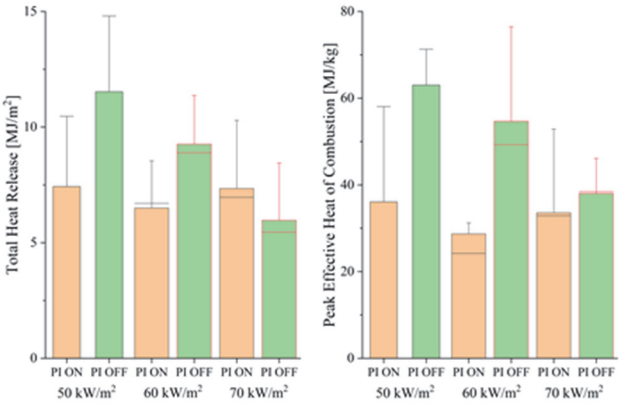

Figure 2 THR and peak EHC values for different heat flux levels and ignition types

3.2 Assessment of Combustion Product/Effluents Composition Depending On Heat Flux Values and Ignition Type

Fig. 3 shows the time-indexed concentration profiles of the identified combustion products/effluents and the HRR curve, enabling comparison of combustion product dynamics with heat release rate changes, while Tab. 3 summarizes their average concentrations and *t*-test results under different conditions. Additionally, in Tab. 3 the results of the two-way ANOVA analysis are shown, examining the effect of heat flux level and ignition type combinations on the concentrations of combustion products.

The two-way ANOVA revealed that heat flux (Factor A) had a statistically significant effect ($p < 0.05$) on all analyzed combustion products, indicating that changes in heat flux levels significantly influence the concentrations of combustion products. Ignition type (Factor B) also shows a statistically significant effect ($p < 0.05$) on the concentrations of most analyzed combustion products (CO, NH_3, NO, NO_2, CH_4, and C_2H_4), indicating that ignition type has a differential influence on combustion product

concentrations. Additionally, the interaction between heat flux (Factor A) and ignition type (Factor B) was statistically significant for all analyzed combustion products, except for H_2O. This also indicates that the interaction between the two factors can have a greater effect on the variation in these concentrations than when each factor is considered individually.

Table 3 Presentation of experimental and statistical results of the interaction between heat flux and ignition type on the concentrations of combustion products/effluents

Heat flux (Factor A)	Ignition type (Factor B)	Combustion products/effluents							
		H_2O / vol%	*t*-test *p*-value	CO_2 / vol%	*t*-test *p*-value	CO / ppm	*t*-test *p*-value	NH_3 / ppm	*t*-test *p*-value
50 kW/m²	PI ON	1.70 ± 0.09	**0.028**	0.89 ± 0.06	**0.000**	7.08 ± 0.53	**0.000**	5.60 ± 0.20	**0.000**
	PI OFF	1.83 ± 0.12		0.57 ± 0.03		17.33 ± 0.61		7.55 ± 0.22	
60 kW/m²	PI ON	1.86 ± 0.09	0.187	0.80 ± 0.03	**0.000**	91.34 ± 4.95	**0.000**	5.02 ± 0.28	**0.000**
	PI OFF	1.91 ± 0.09		0.42 ± 0.02		123.80 ± 6.09		6.35 ± 0.32	
70 kW/m²	PI ON	2.05 ± 0.11	0.796	0.42 ± 0.01	**0.000**	38.35 ± 1.87	0.218	5.65 ± 0.20	**0.000**
	PI OFF	2.02 ± 0.13		1.03 ± 0.07		39.56 ± 1.57		7.31 ± 0.29	
Two-way ANOVA results		***p*-value**		***p*-value**		***p*-value**		***p*-value**	
Heat flux (Factor A)		**0.000**		**0.000**		**0.000**		**0.000**	
Ignition type (Factor B)		0.164		0.059		**0.000**		**0.000**	
Interaction (A × B)		0.231		**0.000**		**0.000**		**0.022**	

Table 3(cont'd)

Heat flux (Factor A)	Ignition type (Factor B)	Combustion products/effluents							
		NO / ppm	*t*-test *p*-value	NO_2 / ppm	*t*-test *p*-value	CH_4 / ppm	*t*-test *p*-value	C_2H_4 / ppm	*t*-test *p*-value
50 kW/m²	PI ON	56.02 ± 3.79	**0.007**	0.21 ± 0.01	**0.000**	0.97 ± 0.05	**0.000**	10.71 ± 0.58	0.386
	PI OFF	46.59 ± 1.96		6.12 ± 0.31		4.75 ± 0.16		11.15 ± 0.58	
60 kW/m²	PI ON	45.64 ± 2	**0.032**	1.05 ± 0.06	**0.000**	10.71 ± 0.52	**0.000**	16.57 ± 1.20	0.378
	PI OFF	41.94 ± 3.10		2.29 ± 0.11		17.46 ± 1.11		16.08 ± 0.70	
70 kW/m²	PI ON	44.70 ± 3.25	0.442	2.52 ± 0.15	**0.002**	3.53 ± 0.18	**0.000**	21.12 ± 1.44	**0.001**
	PI OFF	43.19 ± 1.49		3.08 ± 0.17		6.96 ± 0.46		18.23 ± 0.97	
Two-way ANOVA results		***p*-value**		***p*-value**		***p*-value**		***p*-value**	
Heat flux (Factor A)		**0.000**		**0.000**		**0.000**		**0.000**	
Ignition type (Factor B)		**0.000**		**0.000**		**0.000**		**0.005**	
Interaction (A × B)		**0.004**		**0.000**		**0.000**		**0.000**	

For differences between ignition types at the selected heat flux levels, the t-test revealed statistically significant differences for most combustion products. Exceptions include H_2O at heat fluxes of 60 and 70 kW/m², CO and NO at 70 kW/m², and C_2H_4 at 50 and 60 kW/m².

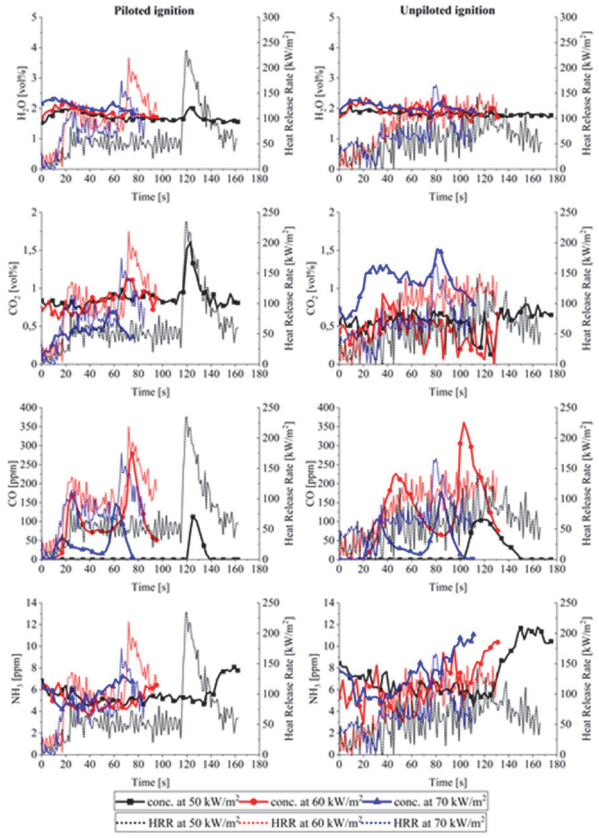

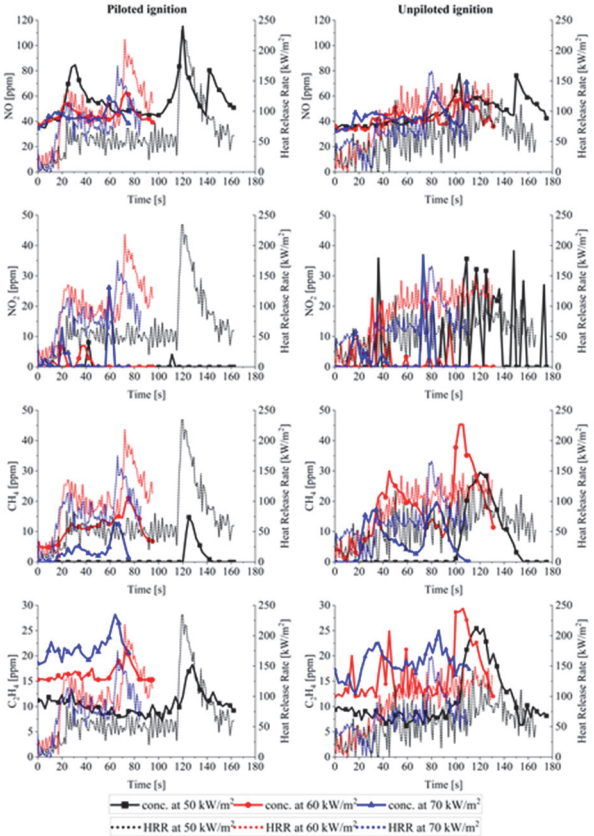

Figure 3 Concentrations of dominant combustion products as a function of time for different ignition types at heat fluxes of 50, 60, and 70 kW/m²

Comparison of the concentration trends of combustion products showed that CO_2, NO, CH_4, and C_2H_4 followed a

similar pattern to the HRR under piloted ignition across all three heat flux levels. These gases also reached their peak concentrations simultaneously with the PHRR. Conversely, under unassisted ignition at a heat flux of 70 kW/m^2, the same gases exhibited a similar trend. However, during the initial combustion phase, their concentrations increased, forming an initial peak before decreasing. At the moment of sample ignition, the concentrations reached their maximum values, coinciding with the PHRR. The trend of water vapor (H_2O) release showed consistency with approximately similar values for both ignition types across all three heat flux levels. A slight increase in concentration was observed under piloted ignition at heat fluxes of 50 and 70 kW/m^2. Compared to unassisted ignition, CO_2 concentrations were significantly higher under piloted ignition across all heat flux levels. This difference is attributed to the formation of a flame during piloted ignition, which promotes more complete combustion, allowing most hydrocarbons to oxidize into carbon dioxide. Piloted ignition resulted in significantly lower CO concentrations compared to unassisted ignition. In contrast, during unassisted ignition, where incomplete combustion is predominant, CO_2 concentrations were lower while CO concentrations were higher, particularly at heat fluxes of 50 and 60 kW/m^2. However, at a heat flux of 70 kW/m^2, both CO_2 and CO concentrations were higher under unassisted ignition, with the differences in CO concentrations between ignition types decreasing. Ammonia (NH_3) was identified as the primary product of the thermal decomposition of nitrogen-containing compounds during combustion. For both ignition types, NH_3 concentrations slightly increased with rising heat flux, especially during the final combustion stages. This trend was more pronounced under unassisted ignition across all three heat flux levels, where higher values and greater fluctuations were recorded. In contrast, the development of NH_3 concentration under piloted ignition was more stable, with smaller variations throughout combustion. NO concentrations were generally higher under piloted ignition due to the higher temperatures achieved, which promote the active thermal dissociation of nitrogen and oxygen, resulting in increased NO formation. Under unassisted ignition, lower temperatures led to slower reaction rates, producing lower NO concentrations [26]. It was also observed that with increasing heat flux, NO concentrations decreased for both ignition types. At an incident heat flux of 50 kW/m^2 under piloted ignition, the maximum NO concentration was identified.

This effect can be explained by the fact that the flame combustion process lasted the longest at a heat flux of 50 kW/m^2 compared to the other experimental trials. Under these conditions, gases remained in the high-temperature zone long enough to facilitate NO formation. At higher heat flux levels, the combustion process was faster, resulting in shorter gas residence times in high-temperature regions. In contrast to NO, NO_2 forms at lower temperatures, typically under conditions of incomplete combustion, which can be clearly identified in the graph. NO_2 concentrations were significantly higher under unassisted ignition, generally increasing with rising heat flux levels in most cases. Methane (CH_4) concentrations, as a significant product of incomplete combustion, showed higher average and peak values under unassisted ignition at heat fluxes of 50 and 60 kW/m^2. At a heat flux of 70 kW/m^2 under unassisted ignition, these values were less pronounced due to sample ignition and partial complete combustion occurring under these conditions. As a consequence of incomplete combustion during unassisted ignition two concentration peaks were noticed, with the second peak being more pronounced and reaching its maximum value during the combustion process. In contrast, under piloted ignition, CH_4 concentrations were more consistent, with a single peak reaching its maximum value while aligning with the development of the PHRR. Furthermore, it was evident that at higher heat flux levels (70 kW/m^2), CH_4 concentrations decreased. A similar trend was observed for ethylene (C_2H_4) concentrations, with higher peak values recorded under unassisted ignition at heat fluxes of 50 and 60 kW/m^2. Similarly, the variation in maximum ethylene (C_2H_4) levels between piloted and unassisted ignition diminished at a heat flux of 70 kW/m^2 mirroring the trends observed with carbon monoxide (CO) levels.

3.3 PCA Analysis Results of Flammability Parameters and Combustion Product Composition Depending on the Ignition Type

Principal Component Analysis (PCA) was conducted to assess the interrelationships between flammability parameters and combustion products under different heat flux levels (50, 60, and 70 kW/m^2) and ignition types (piloted and unassisted ignition). Figs. 4, 5, and 6 present PCA biplots for each individual heat flux, illustrating the influence of ignition type on the interdependence between flammability parameters and combustion products. For all three heat flux levels, the two ignition types were well separated on the biplot, highlighting their distinct combustion characteristics. PCA biplots provide a clear overview of the variability in the data, allowing for the detection of significant trends and relationships between different variables. The following section presents the analysis of PCA biplots by heat flux level.

PCA biplot analysis for a heat flux of 50 kW/m^2

At a heat flux of 50 kW/m^2, the first principal component (PC1) explained 76.97% of the variance, while the second component (PC2) accounted for 9.73%, resulting in a cumulative variance of 86.7% (Fig. 4). This indicated that most of the variability in the dataset was attributed to the first dimension, making it the dominant component. The experimental group of samples subjected to piloted ignition (PI_ON) was more closely associated with variables oriented on the negative side of the first principal component (PC1), such as PHRR, mean HRR, MLR, and CO_2 concentrations. These variables exhibited higher values in samples exposed to piloted ignition (PI_ON), further indicating that piloted ignition led to more intense combustion, characterized by higher heat release rates and a faster combustion process. Additionally, CO_2 emissions followed the same trend, suggesting more complete combustion under piloted ignition conditions.

On the other hand, on the positive side of the first principal component (PC1), the experimental group of samples subjected to non-piloted ignition (PI_OFF) was characterized by higher values of THR and peak EHC, as

well as increased emissions of gases such as CO, NH_3, NO_2, and CH_4. This indicated that non-piloted ignition resulted in a lower combustion intensity but simultaneously led to higher concentrations of gases associated with incomplete combustion, suggesting a less efficient combustion process. Since no ignition occurred in the samples at a heat flux of 50 kW/m^2, the TTI was not measured. As a result, this variable was oriented towards the positive side of the first principal component (PC1), in the region where the samples subjected to non-piloted ignition (PI_OFF) were located. On the other hand, the variables H_2O and C_2H_4 were dominant on the positive side of the second principal component (PC2). Their position suggested that the application of piloted ignition did not significantly affect the differences in the concentrations of these gases. MLR had similar coefficients for PC1 and PC2. However, since PC1 accounted for a significantly larger variance, this variable was primarily associated with higher heat release rates in samples subjected to piloted ignition (PI_ON). THR and peak EHC also had similar coefficients for PC1 and PC2. However, they were not exclusively linked to PC1 but contributed significantly to the second principal component (PC2) as well.

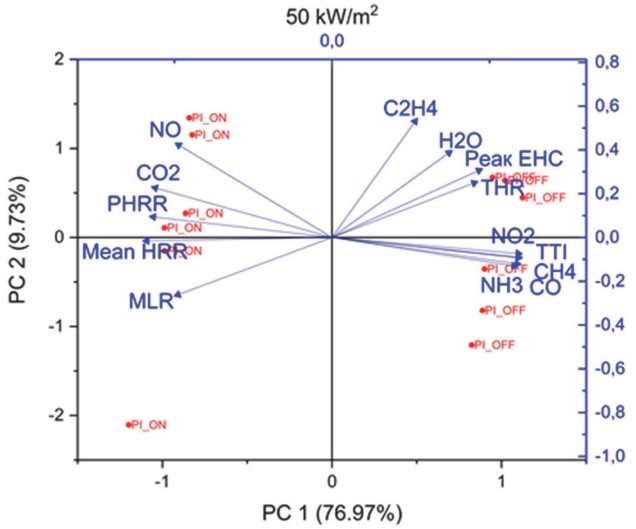

Figure 4 Biplot showing the correlation between flammability parameters and combustion products depending on the ignition type at a heat flux of 50 kW/m^2

PCA biplot analysis for a heat flux of 60 kW/m^2

Comparing the PCA results obtained at heat fluxes of 50 and 60 kW/m^2, certain similarities could be observed. At a heat flux of 60 kW/m^2, the two main dimensions, PC1 and PC2, explained 71.20% and 9.35% of the variance, respectively, resulting in a cumulative variance of 80.55% (Fig. 5).

Similar to the heat flux of 50 kW/m^2, the distribution of flammability parameters and combustion products at a heat flux of 60 kW/m^2 clearly reflected the differences between samples subjected to different ignition types, with a few key differences in the distribution of variables and their influence on the PCA dimensions. Here MLR had a greater influence on the second dimension (PC2), indicating that this variable increasingly depended on other factors not exclusively related to the ignition type. Additionally, the concentration of H_2O showed an even stronger correlation with the second dimension (PC2), confirming that the application of piloted ignition was not a dominant factor in water vapor concentration. Furthermore, the position of TTI remained unchanged, confirming the previously stated findings. Additionally, unlike the results at a heat flux of 50 kW/m^2, THR and peak EHC were primarily associated with the first dimension (PC1) at a heat flux of 60 kW/m^2. This indicated that their influence depended on the intensity of heat release in samples subjected to non-piloted ignition (PI_OFF).

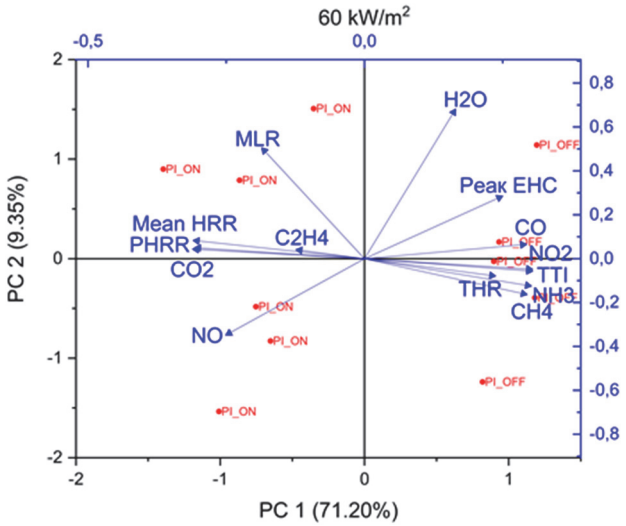

Figure 5 Biplot showing the correlation between flammability parameters and combustion products depending on the ignition type at a heat flux of 60 kW/m^2

PCA biplot analysis for a heat flux of 70 kW/m^2

At a heat flux of 70 kW/m^2, the first principal component (PC1) accounted for 38.56% of the variance, while the second component (PC2) explained 23.75%, resulting in a cumulative variance of 62.31% in the dataset (Fig. 6). Compared to lower heat fluxes (50 and 60 kW/m^2), the contribution of the first dimension (PC1) was significantly lower, indicating that the second dimension (PC2) played a more substantial role in differentiating the samples. The experimental group of samples subjected to piloted ignition (PI_ON) was primarily positioned on the negative side of the first principal component (PC1) and was closely associated with higher concentrations of ethylene (C_2H_4) and moderately increased concentrations of NO. This distribution of variables indicated that the samples exposed to piloted ignition (PI_ON) at 70 kW/m^2 underwent more intense pyrolysis processes, leading to greater releases of C_2H_4 and NO, that was formed during high-temperature oxidation. The NO variable had similar coefficients for PC1 and PC2, and since PC1 carried a greater variance, this variable was primarily associated with samples subjected to piloted ignition (PI_ON).

On the other hand, on the positive side of the first principal component (PC1), samples subjected to non-piloted ignition (PI_OFF) were grouped, characterized by higher concentrations of CH_4, CO_2, NH_3, and NO_2, as well as longer ignition times (TTI).

The PHRR, mean HRR, MLR, as well as the gases H_2O and CO, were dominant on the positive side of the second principal component (PC2). Reversely, the THR and peak EHC were positioned on the negative side of the second principal component (PC2). As ignition occurred at a heat flux of 70 kW/m^2 even under non-piloted ignition conditions (meaning spontaneous ignition happened), the

analysis of the variable positions within the second dimension (PC2) indicated that samples with higher heat release rates (PHRR and mean HRR) exhibited lower values of THR and peak EHC. This could have been a consequence of shorter combustion duration, accompanied by higher peak and mean heat release rates, leading to reduced THR and peak EHC. This trend suggested that as the heat flux increased and reached the threshold for spontaneous ignition, the influence of ignition type on variations in these variables became less pronounced. Instead, they primarily depended on secondary factors such as pyrolysis, thermal degradation mechanisms, and the physicochemical properties of the samples.

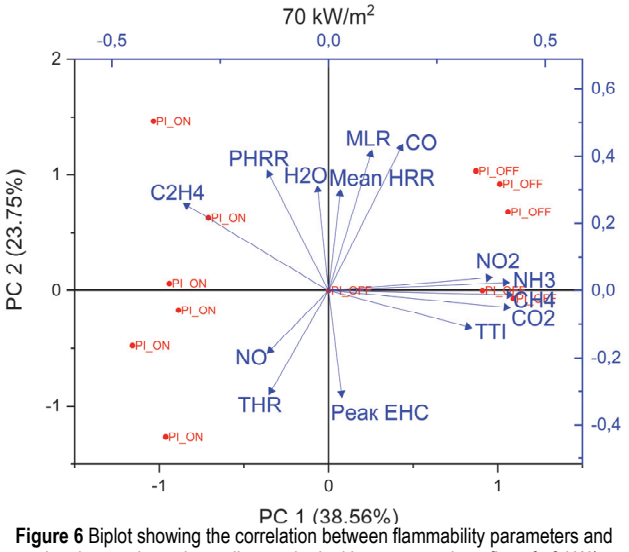

Figure 6 Biplot showing the correlation between flammability parameters and combustion products depending on the ignition type at a heat flux of 70 kW/m²

4 CONCLUSION

This study investigated the influence of ignition type (piloted and unassisted) on the combustion dynamics and combustion products/effluents of live terminal branch samples of *Pinus nigra* while they were exposed to three heat flux levels (50, 60, and 70 kW/m^2). Experiments were performed on an adapted mass loss calorimeter coupled with an FTIR gas analyzer for real-time characterization of effluents.

Under piloted ignition, the development of a flame phase was observed at all heat flux levels. In contrast, under unassisted ignition, smouldering combustion occurred at heat fluxes of 50 and 60 kW/m^2. However, at a heat flux of 70 kW/m^2, without the use of a spark igniter, the samples ignited and maintained a steady flame.

The use of piloted ignition resulted in a shorter time to ignition (TTI) which can be directly attributed to the presence of the spark igniter. Additionally, the spark igniter enabled faster initiation of the flaming phase, leading to higher average and peak heat release rates (PHRR) and a reduced time to reach these values. In contrast, unassisted ignition was characterized by slower energy release, resulting in lower heat release rates at heat fluxes of 50 and 60 kW/m^2. However, at a heat flux of 70 kW/m^2, the differences between piloted and unassisted ignition became minimal, indicating that the radiant energy from the instrument‘s conical heater was sufficient to initiate effective flaming combustion even without the spark igniter. We also found that at heat fluxes of 50 and 60 kW/m^2, unassisted ignition resulted in higher total heat release (THR) values compared to piloted ignition.

The interaction between different heat flux levels and ignition type significantly influenced the concentrations of combustion products. The concentrations of CO_2, NO, CH_4, and C_2H_4 followed the heat release rate (HRR) trends across all three heat flux levels during piloted ignition and at 70 kW/m^2 under unassisted ignition conditions. Piloted ignition was characterized by more complete combustion and higher temperatures, resulting in elevated concentrations of carbon dioxide (CO_2) and nitric oxide (NO), along with lower concentrations of carbon monoxide (CO) and methane (CH_4) compared to unassisted ignition. This difference was particularly pronounced at heat fluxes of 50 and 60 kW/m^2. At a heat flux of 70 kW/m^2, unassisted ignition led to the formation of a flame phase, which minimized concentration differences between the two ignition types for most combustion products, except for H_2O, CO, and NO.

Finally, the obtained results highlight the significant role of ignition type in combustion dynamics, especially regarding the rate at which the peak heat release rate (PHRR) is achieved which is a key element in fire behavior research.

The results obtained in our study have several potential practical applications. The first contribution is the provision of ignition-limit data that can be used to validate physics-based components in emerging coupled fire–atmosphere models (e.g., CFBM-UFS), and to calibrate empirical rate-of-spread systems that still rely on legacy ignition coefficients. Moreover, because every heat-flux/ignition-mode condition in our experiments was accompanied by time-resolved in situ FTIR spectroscopic characterization of the evolving combustion gases, the resulting dataset can be readily converted into fuel- and mechanism-specific emission factors for use in air-quality and greenhouse-gas inventories. Finally, from an operational perspective, the finding that radiant fluxes $\geq$ 70 kW/m^2 eliminate the need for a pilot suggests that fire-behaviour analysts may use remote-sensing-derived radiant heat maps to distinguish areas where ignition is primarily radiation-driven. In such zones, ember mitigation measures may be deprioritized, allowing suppression resources targeting ember-induced ignitions to be more effectively allocated to areas with sub-critical flux levels.

Acknowledgements

This work was financially supported by the Ministry of Science, Technological Development and Innovation of the Republic of Serbia [Grants No.:451-03-137/2025-03/200148 -SDGs Goal 13, 451-03-136/2025-03/200052 and 451-03-136/2025-03/200017] and ERASMUS+ Jean Monnet Module "Workplace and Process Safety in Next Generation Europe - Teaching for Learning".

5 REFERENCES

[1] Radeloff, V. C., Helmers, D. P., Anu Kramer, H., Mockrin, M. H., Alexandre, P. M., Bar-Massada, A., Butsic, V., Hawbaker, T. J., Martinuzzi, S., Syphard, A. D., & Stewart, S. I. (2018). Rapid growth of the US wildland-urban

interface raises wildfire risk. *Proceedings of the National Academy of Sciences of the United States of America*, *115*(13), 3314-3319. https://doi.org/10.1073/pnas.1718850115

[2] Gincheva, A., Pausas, J. G., Edwards, A., Provenzale, A., Cerdà, A., Hanes, C., Royé, D., Chuvieco, E., Mouillot, F., Vissio, G., Rodrigo, J., Bedía, J., Abatzoglou, J. T., Senciales González, J. M., Short, K. C., Baudena, M., Llasat, M. C., Magnani, M., Boer, M. M., … Turco, M. (2024). A monthly gridded burned area database of national wildland fire data. *Scientific Data*, *11*(1), 352. https://doi.org/10.1038/s41597-024-03141-2

[3] Yue, X., Mickley, L. J., Logan, J. A., & Kaplan, J. O. (2013). Ensemble projections of wildfire activity and carbonaceous aerosol concentrations over the western United States in the mid-21st century. *Atmospheric Environment*, *77*, 767-780. https://doi.org/10.1016/j.atmosenv.2013.06.003

[4] Rothermel, R. C. (1972). *A mathematical model for predicting fire spread in wildland fuels*. Department of Agriculture, Intermountain Forest and Range Experiment Station.

[5] "BehavePlus" https://research.fs.usda.gov/firelab/products/dataandtools/software/behaveplus

[6] "FlamMap" https://research.fs.usda.gov/firelab/products/dataandtools/software/flammap

[7] "FireFamily" https://research.fs.usda.gov/firelab/products/dataandtools/software/firefamilyplus

[8] Blauw, L. G., Wensink, N., Bakker, L., van Logtestijn, R. S. P., Aerts, R., Soudzilovskaia, N. A., & Cornelissen, J. H. C. (2015). Fuel moisture content enhances nonadditive effects of plant mixtures on flammability and fire behavior. *Ecology and Evolution*, *5*(17), 3830-3841. https://doi.org/https://doi.org/10.1002/ece3.1628

[9] de Magalhães, R. M. Q., & Schwilk, D. W. (2012). Leaf traits and litter flammability: Evidence for non-additive mixture effects in a temperate forest. *Journal of Ecology*, *100*(5), 1153-1163. https://doi.org/10.1111/j.1365-2745.2012.01987.x

[10] Chiaramonti, N., Romagnoli, E., Santoni, P. A., & Barboni, T. (2017). Comparison of the Combustion of Pine Species with Two Sizes of Calorimeter: 10 g vs. 100 g. *Fire Technology*, *53*(2), 741-770. https://doi.org/10.1007/s10694-016-0595-1

[11] Mutch, R. W. (1964). Ignition delay of ponderosa pine needles and sphagnum moss. *Journal of Applied Chemistry*, *14*(7), 271-275. https://doi.org/https://doi.org/10.1002/jctb.5010140702

[12] Popović, Z., Bojović, S., Marković, M., & Cerdà, A. (2021). Tree species flammability based on plant traits: A synthesis. *Science of the Total Environment*, *800*. https://doi.org/10.1016/j.scitotenv.2021.149625

[13] Jaureguiberry, P., Bertone, G., & Díaz, S. (2011). Device for the standard measurement of shoot flammability in the field. *Austral Ecology*, *36*(7), 821-829. https://doi.org/10.1111/j.1442-9993.2010.02222.x

[14] Wyse, S. V., Perry, G. L. W., O'Connell, D. M., Holland, P. S., Wright, M. J., Hosted, C. L., Whitelock, S. L., Geary, I. J., Maurin, K. J. L., & Curran, T. J. (2016). A quantitative assessment of shoot flammability for 60 tree and shrub species supports rankings based on expert opinion. *International Journal of Wildland Fire*, *25*(4), 466-477. https://doi.org/10.1071/WF15047

[15] Alam, M. A., Wyse, S. V., Buckley, H. L., Perry, G. L. W., Sullivan, J. J., Mason, N. W. H., Buxton, R., Richardson, S. J., & Curran, T. J. (2020). Shoot flammability is decoupled from leaf flammability, but controlled by leaf functional traits. *Journal of Ecology*, *108*(2), 641-653. https://doi.org/10.1111/1365-2745.13289

[16] Frejaville, T., Curt, T., & Carcaillet, C. (2013). Bark flammability as a fire-response trait for subalpine trees. *Frontiers in Plant Science*, *4*. https://doi.org/10.3389/fpls.2013.00466

[17] Grootemaat, S., Wright, I. J., van Bodegom, P. M., Cornelissen, J. H. C., & Shaw, V. (2017). Bark traits, decomposition and flammability of Australian forest trees. *Australian Journal of Botany*, *65*(4), 327-338. https://doi.org/10.1071/BT16258

[18] Plucinski, M. P. & Anderson, W. R. (2008). Laboratory determination of factors influencing successful point ignition in the litter layer of shrubland vegetation. *International Journal of Wildland Fire*, *17*(5), 628-637. https://doi.org/10.1071/WF07046

[19] Guillaume, B., Ganteaume, A., Majeri, M., Fayad, J., El Houssami, M., Pizzo, Y., & Porterie, B. (2025) New Laboratory Results on Ignition and Propagation in Live Vegetation Paving the Road to a Semi-Empirical Model. *Fire and Materials*. https://doi.org/https://doi.org/10.1002/fam.3273

[20] Lobert, J. & Warnatz, J. (1993). Emissions from the combustion process in vegetation. *Fire in the Environment*, *13*.

[21] Ma, Y., Yang, S., Zhu, Z., Wang, G., Tigabu, M., Guo, Y., Zheng, W., & Guo, F. (2022). Emissions of gaseous pollutants released by forest fire in relation to litter fuel moisture content. *Atmospheric Environment*, *284*, 119215.

[22] May, N., Ellicott, E., & Gollner, M. (2019). An examination of fuel moisture, energy release and emissions during laboratory burning of live wildland fuels. *International Journal of Wildland Fire*, *28*(3), 187-197. https://doi.org/10.1071/WF18084

[23] Protić, M., Mišić, N., Tasić, V., & Božilov, A. (2025). Heat flux impact on live *Pinus nigra* branches and characterization of gaseous emissions. *Proceedings of the Ninth International WeBIOPATR Workshop & Conference: Particulate Matter: Research and Management*, 117-123.

[24] *ISO 5660-1 Reaction-to-fire tests - Heat release, smoke production and mass loss rate Part 1: Heat release rate (cone calorimeter method) and smoke production rate (dynamic measurement)*, 2015.

[25] Protić, M., Mišić, N., Raos, M., Mančić, M., & Popović, M. (2024). Overview of Common Methods for Fire Testing. *Facta Universitatis, Series: Working and Living Environmental Protection*, *21*(1), 19-35.

[26] Paul, K. T., Hull, T. R., Lebek, K., & Stec, A. A. (2008). Fire smoke toxicity: The effect of nitrogen oxides. *Fire Safety Journal*, *43*(4), 243-251. https://doi.org/https://doi.org/10.1016/j.firesaf.2007.10.003

Contact information:

Milan PROTIĆ, PhD, Associate Professor
(Corresponding author)
University of Niš, Faculty of Occupational Safety,
Čarnojevića 10A, 18000 Niš, Serbia
E-mail: milan.protic@znrfak.ni.ac.rs

Nikola MIŠIĆ, MSc, Teaching Assistant
University of Niš, Faculty of Occupational Safety,
Čarnojevića 10A, 18000 Niš, Serbia
E-mail: nikola.misic@znrfak.ni.ac.rs

Miomir RAOS, PhD, Full Professor
(Corresponding author)
University of Niš, Faculty of Occupational Safety,
Čarnojevića 10A, 18000 Niš, Serbia
E-mail: miomir.raos@znrfak.ni.ac.rs

Viša TASIĆ, PhD, Principal Research Fellow
Mining and Metallurgy Institute Bor,
Alberta Ajnštajna 1, 19210 Bor, Serbia
E-mail: visa.tasic@irmbor.co.rs

Dušan TOPALOVIĆ, PhD, Research Associate
Vinča Institute of Nuclear Sciences-National Institute of the Republic of Serbia,
University of Belgrade
Mike Petrovića Alasa 12-14, 11000 Belgrade
E-mail: dusan.topalovic@vin.bg.ac.rs